

# Response of the African Equatorial-Low Latitudes Ionosphere to 17 March 2013 and 01 June 2013 Geomagnetic Storms

Mustapha Abbas<sup>1,\*</sup>, Mukhtar Mohammad<sup>2</sup>, Mukhtar Ibrahim Furfuri<sup>1,3</sup>, Asabe Ibrahim Audu<sup>2</sup>, Mohammed Bello Kaoje<sup>1</sup>Arzika Yusuf Koko<sup>1, 4</sup>, Aminu Muhammad<sup>1</sup>

- 1. Department of Physics, Kebbi State University of Science and Technology, Aliero, Nigeria
  - 2. Department of Physics, Federal University of Agriculture, Zuru,-Kebbi State, Nigeria
- 3. Department of Physics, Federal College of Education Technical, Gusau, Zamfara State, Nigeria
  - 4. Department of Physics, Federal University of Education, Kotangora, Niger State, Nigeria E-mail of the corresponding author: <a href="mailto:maphysik@yahoo.com">maphysik@yahoo.com</a>

## **Abstract**

Response of the equatorial-low latitude ionosphere to the moderate storms of 17 March 2013 (Dst min=130 nT) and 1 June, 2013 (Dst min=137 nT) has been investigated using GPT-TEC observations in the African sector. The result shows significant response of the GPS-TEC to the two magnetic storm events particularly during the main and recovery phases of the storm. Series of negative and positive responses were observed in the two magnetic storms. The study reveals that for both magnetic storms, the occurrence of SSC associated with northward turning of some magnetic and interplanetary parameters mostly do not produce any significant deviation between the storm-time and mean quiet-time TEC at the equatorial-low latitude around (06:00-11:00) UT hrs. For the 1 June magnetic storm, negative storm-time effect were mostly observed around (06:00-11:00) UT hrs across all the latitudes during the main and recovery phases of the storm. Similar variations are mostly observed during the main and recovery phases of the magnetic storms. However, series of negative and positive storm-time effects were observed in the two magnetic storms. During the main phase, both storms exhibit faint positive storm-time effect around (12:00-14:00) UT hrs across most of the latitudes. During the recovery phase, a faint positive storm-time effect are observed around (06:00-11:00) UT hrs in most latitudes during the March magnetic storm and reverse is the case for the June storm event. The main phase negative storm-time are consequences of weaker PPEF and negative storm-time effect during the recovery phase is a strong evidence of predominance of ionospheric disturbance dynamo electric field (DDEF) suppressing the fountain effect.

Keywords: Ionosphere, Geomagnetic field, electric field, magnetic storm

DOI: 10.7176/APTA/89-04

Publication date:October 31st 2025

#### 1. Introduction

The combine effect of coronal mass ejection (CMEs) and the emission of high speed solar wind stream (HSSWS) causes temporary disturbance magnetosphere-ionosphere current system globally known as geomagnetic storm, Imitiaz et al., 2020. A typical geomagnetic storms are usually characterized by three distinguished phases after the storm sudden commencement (SSC): the initial phase, main and recovery phases [e.g., Gonzalez et al., 1994; Prolss, 1995]. At each phase of the magnetic storm, energy is deposited in the ionosphere and this alters the chemical and electrodynamics configuration of the ionosphere Liu et al., 2010. The energy deposition is maximum at the main phase of the storm, decreases through the recovery phase Schunk and Nagy, 2000; Richmond and Liu, 2000. Moreover, at each particular phase, the response of the ionosphere to the energy deposition is dependent on latitude, season, local time and geophysical conditions during the storm Gonzalez et al., 1994. The dawn-dusk Interplanetary Electric Field (IEF) associated with energy interactions influences the ionosphere, generating drifts and changes in ionospheric parameters such as electron density, total electron content (TEC) and magnetic field intensity among others. Two physical phenomenon acting at a planetary scale contribute to the storm-time behavior of the equatorial-low latitude ionosphere: the prompt penetration electric fields (PPEFs) as previously pointed out by Spiro et al., 1988 and the ionospheric disturbance dynamo electric field (DDEF) caused by the global thermospheric wind circulation associated with joule heating at high latitudes Blanc and Richmond, 1980. The presence of prompt penetration electric field (PPEF) and ionospheric disturbance dynamo electric field (DDEF) causes large perturbations in the zonal electric field which significantly modifies the behavior of the TEC and equatorial ionization anomaly (EIA), thereby resulting in severe ionospheric changes at equatorial-low latitudes e.g., Abdu et al., (1991). The under-shielding/over-shielding associated with the orientation of the interplanetary magnetic field (Bz) are eastward/westward during the daytime and westward/eastward during the night-time. Huang et al. 2005 explained that when the (IMF) Bz is southward, the PPEFs intensifies the plasma fountain effect hence, more plasma will be transported to a height with minimal loss rate, Lin et al., 2005; Zhao et al., 2005. Fagundes et al. 2016 and Akala et al. 2020 further explained that the northward (westward) orientation of the



PPEFs during magnetic storms cause reversal of fountain effect leading to reduction in ionospheric total electric content (TEC). This implies that the orientation of the PPEFs changes the overall behavior of the EXB drift which causes significant TEC deviation from its quiet-time behavior during the main and recovery phases of a magnetic storm. The deviation of TEC either by increase or decrease relative to the quiet-time lead to positive or negative ionospheric storm-time effect Wang et al., 2010.

It is now certain that every geomagnetic storm exhibit different features and behavior of the EXB plasma drift thereby result to either increase or decrease in TEC with reference to the quiet day or pre-storm periods. Since the response of the ionospheric TEC varies from one geomagnetic storm to the other as a result of the variations of some mechanism. It becomes imperative to study the ionospheric effect in each geomagnetic storm so as to have better understanding of the physical and electrodynamics mechanisms that are involve during geomagnetic storm. Radio communication systems that depend on ionosphere are distorted during geomagnetic storms Moore et al., 1999. High-frequency (HF) radio signals are sometimes distorted in the ionosphere thereby affecting long-distance radio communication by changing the path and velocity of radio waves, Shishir et al., 2016; Laura et al., 2017. Also, during geomagnetic storms radio signals from GPS satellites passing through the ionosphere may experience delays and errors in signal propagation which adversely lead to inaccuracies in GPS position estimates, hence affecting navigation and timing applications. Hence, understanding the storm-time response is very crucial and most often times complex due to varying characteristics and the local conditions at the region of interest. In this paper, we have considered two distinct geomagnetic storms which exhibit some level of similarities at one point and differs in their interplanetary and geomagnetic conditions. On this note, the remainder of this study is organized in the following ways: section 2 present a brief description of the source of data and the analysis procedure. Presented in section 3 is the result of the study and discussion and finally we draw conclusion in section 4.

## 2. Data Sources and Method of Analysis

The study was carried out using total electron content (TEC) obtained from global positioning system (GPS) located at the equatorial-low latitude region of Africa. Two moderate geomagnetic storms that occurred on 17 March and 1 June, 2013 were selected for this study. To examine the response of the ionosphere to each of the geomagnetic storm, we choose 2 days prior to the occurrence of the geomagnetic storm so as to study the characteristics of the storms before the occurrence of the storm sudden commencement (SSC). To identify whether the magnetic storm creates a positive or negative storm-time effect, we use 3 days GPS-TEC data whose  $Kp \le 4$  within the month of the occurrence of the magnetic storm to compute the mean quiet-time TEC variations. This was achieved by simply taking the average of all the quietest days with  $Kp \le 4$  within the month in which the magnetic storm occurred. Figure 1 show the locations of the GPS stations where the TEC data were obtained Originally, the GPS-TEC data are recorded in the Receiver Independent Exchange (RINEX) format obtained from www.unavco.org/data/gpsgnss/dataccessm ethods/dai 2/html.

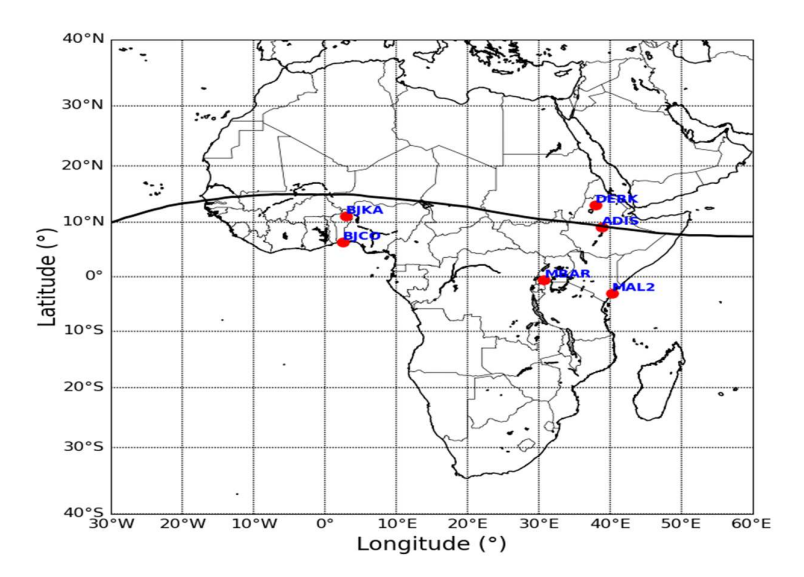


Figure 1 Locations of the GPS stations used on the African Map



The data which was originally in RINEX format were processed through the GPS-TEC analysis program developed by Seemala and Valladares, 2011; Seemala *et al.*, 2023. Thus, to have a comprehensive understanding of the latitudinal response of the TEC to geomagnetic storms and its impact on navigation and other technological systems, we engaged 6 GPS-TEC stations across equatorial-low latitudes in Africa. The solar wind, interplanetary and geomagnetic indices used in the study were obtained from Omni web accessible at <a href="https://omniweb.gsfc.nasa.Gov/cgi/">https://omniweb.gsfc.nasa.Gov/cgi/</a> nx1.cgi.

## 3 Results and Discussion

### 3.1. The 17 March, 2013 Geomagnetic storm event

The temporal variations of interplanetary and magnetic parameters from 15 to 20 March 2013 are illustrated in Figure 2 in the following order from top to bottom: interplanetary magnetic field (IMF) Bz, solar wind speed V, dynamic pressure (PSW), interplanetary electric field (IEFy), disturbance storm time (Dst), Ap index and auroral electrojet (AE) index. Prior to the occurrence of the magnetic storm, NASA reported an eruption of a magnetic filament which produces M1-class solar flare and a bright CME directly towards the Earth. The CME hit the Earth's magnetic field at 06:04 UT on 17 March 2013. The impact caused tremendous increase in solar wind speed V from 400 km/s to about 700 km/s (see Figure 2 panel b). The magnetic storm started with the outer compression of the magnetosphere which manifest as a sharp increment in dynamic pressure to a maximum value ~13 nPa marked by the storm sudden commencement (SSC) at 06:04 UT on 17 March 2013 as illustrated in Figure 2 (panel c). The initial phase of the storm lasted for about 1 hr of which the Bz depicted in Figure 2 (panel a) and the speed V and Dst index in panels c and e remained northward. Shortly after these features, the Bz and Dst index turned southward marking the onset of the main phase of the magnetic storm which begins around 07:00 UT on 17 March 2013. The Dst index exhibit a systematic reduction during the main phase with two minima  $\sim -100$  nT at 10:30 UT and the second minima  $\sim -132$  nT at 20:30 UT all on 17 March 2013. These two distinct minimum values characterized the main phase of the storm that lasted for 14 hrs. During the main phase of the storm, Bz remained strongly southward (see Figure 2 panel a) indication of possible prompt penetration electric field (under-shielding) resulting to sudden increase in the dawn side convection electric field at high latitudes as earlier established by Nishida 1968; Sastri et al., 1992; Kikuchi et al., 2008. Fejer et al. 1990 observed that the under-shielding electric field penetrates instantly to the equatorial-low latitude region exhibiting eastward (westward) polarity during the daytime (night-time) periods. The southward orientation of Bz during the main phase of the storm is accompanied by a northward fluctuation of IEFy lasting for several hours (see Figure 2 panel d). The IEFy reached its maximum amplitude ~10 mV/m on 17 March 2013 and fluctuate thereafter similar to what was observed in the Bz. These variations indicate significant perturbations in the electrodynamic processes of the upper atmosphere. During the main phase of the storm, V increase significantly from ~350 km/s to about 720 km/s as shown in Figure 2 (panel b) and thereafter decreases through the recovery phase. The perturbations in IEFy (panel d), AE (panel g) and Ap index (panel f) during the main phase shows that significant amount of energy may be penetrating the thermosphere-ionosphere system during these periods. It is interesting to note that the initial and main phases of the geomagnetic storm of 17 March 2013 occurred during the local daytime with the main phase extending to the local midnight hours. The response of the (IMF) Bz, dynamic pressure (PSW), oscillations in the interplanetary electric field (IEFy) and the auroral activity (AE) indicate the strong penetration of highly energy particles into the ionosphere around 10:30 UT on 17 March, 2013 and lasted for about 14 hrs.



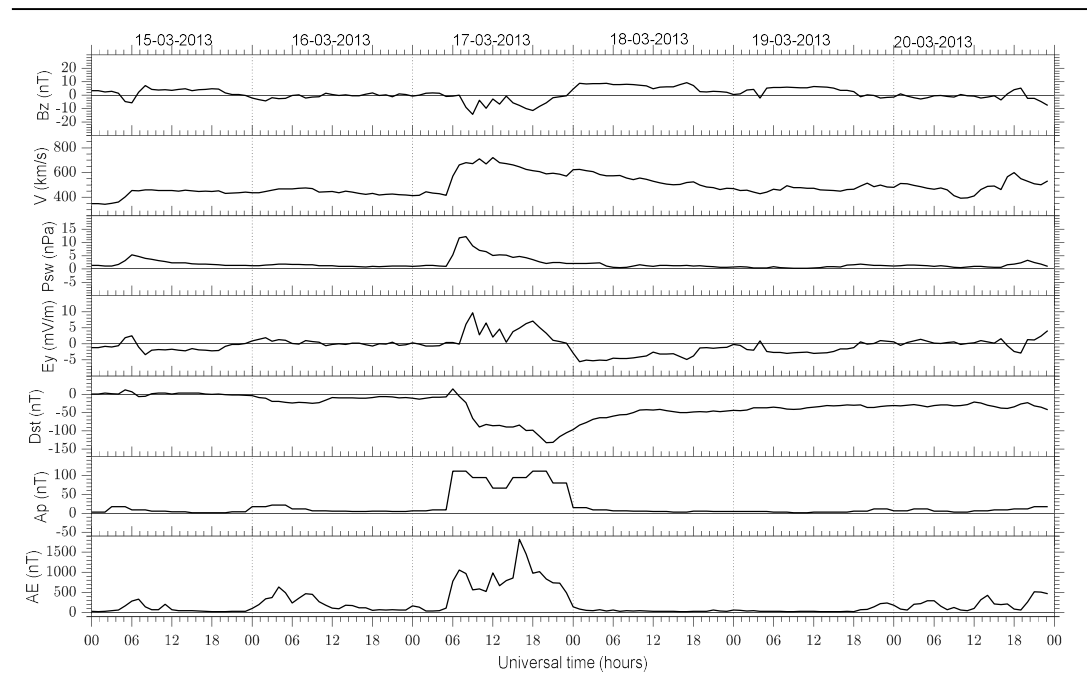


Figure 2 interplanetary magnetic field, and geomagnetic activity indices during the March 17 2013 geomagnetic storm. From top to bottom are the interplanetary magnetic field (IMF) Bz, solar wind speed (Vx) dynamic pressure (PWS), Interplanetary electric field (IEF), disturbance storm time (Dst), Ap index, and auroral electrojet (AE).

The recovery phase of the storm started around 21:30 UT on 17 March 2013 marked by the northward turning of Bz indication of possible over shielding penetration electric field effect. During these periods, the Bz remained relatively northward obviously seen on 18 March 2013 (see Figure 2 panel a) associated with a downward decrease in V and a positive increase in Dst values as depicted in Figure 2 (panel b and c). In fact, during the recovery period, all the parameters return to their normal levels signaling the absence of any form of major disturbances in the electrodynamic process of the thermosphere-ionosphere system.

## 3.2 Ionospheric Total Electron Response to the 17 March 2013 Geomagnetic storm event

Figure 3 illustrates the storm-time diurnal variations of TEC and their comparison with the mean quiet-time TEC variations over African equatorial-low latitudes during the 15-20 March 2013 magnetic storm. The GPS-TEC stations are presented in different rows in the increasing order of geomagnetic latitude from top to bottom namely: AAB, BJKA, BJCO, DEBK, MAL2 and MBAR respectively. The blue line represents the mean quiet-time TEC obtained from the average of 3 quietest days with Kp≤4 prior to the occurrence of the storm and the black line represents the storm-time TEC variation. The mean quiet-time TEC variations are taken as the reference field such that when the storm-time TEC magnitude is more (less) than the mean quiet-time TEC magnitude, it is recognized as positive (negative) storm-time effect Lin et al., 2005; Fagundes et al., 2016; Akala et a., 2020. This criterion has been adopted throughout this study and thus helps identify the ionospheric positive and negative storm time effect. It is evident in Figure 3 that 2 days before the SSC (15-16 March 2013), the mean quiet-time TEC exhibit similar trend and magnitude with the storm-time TEC around (06:00-11:00) UT across all the latitudes indication of absence of any significant disturbances between the mean quiet-time TEC variations obtained from 3 quietest days and the daily storm-time TEC during these periods. A slight deviation is observed between the storm-time TEC and the mean quiet-time TEC variations around noontime (12:00-14:00) UT hrs that are more prevalent at BJKA, BJCO and DEBK latitudes before the occurrence of SSC (15-16 March 2013). We assert that these deviations may likely reflect variations in electrodynamic processes and the effective distribution of the fountain effect. Shortly after these features, a significant night-time (19:00-20:00) UT enhancement that seems to increase with geomagnetic latitude is seen during the storm-time and mean quiet-time TEC variations on 15-16 March 2013. These night-times TEC enhancement may likely be associated with pre-reversal enhancement (PRE) Abbas et al., 2024.

On the day of the storm (17 March 2013), the storm-time and mean quiet-time TEC exhibit almost equal magnitude and trend around (06:00-11:00) UT hrs across all the latitudes. During these periods, the SSC that is marked by a northward orientation of Dst index, dynamic pressure (PSW) and V lasting for about 1 hr do not cause any



significant effect on the diurnal variation of the storm-time TEC during the dawn sector (06:00-11:00) UT hrs. This further shows that for the SSC that occurred around 06:04 UT on 17 March, 2013 associated with northward turning of some interplanetary parameters do not produce any significant effect on the TEC variations in the African equatorial-low latitude regions around (06:00-11:00) UT. The storm day (17 March 2013) which coincides with the main phase of the storm associated with a southward orientation of Bz, Dst index and northward increase in IEFy, the storm-time TEC magnitudes were observed to be higher than the mean quiet-time around (12:00-14:00) UT hrs. These features are conspicuously seen across all latitudes. The perturbations in the auroral electrojet (AE) index, southward turning of Bz and Dst index accompanied by a northward IEFy during the main phase of the storm (17 March 2013) show an episode of enhanced energy deposition at high latitudes. The presence of eastward PPEF generally modifies the zonal eastward electric field which generates positive storm-time effect across all the latitudes around (12:00-14:00) UT hrs Huang et al., m 2005; Fagundes et al., 2016, Akala et al., 2020. It is worthy to note that during the main phase, the prompt penetration electric field is predominantly eastward and this caused incredible enhancement in the dynamo electric field which in-turn enhance the vertical EXB plasma drift which transport the ionospheric plasma to height with minimal loss rate that results to positive storm-time effect around (12:00-14:00) UT hrs of this present study. Amazingly, MAL2 and MBAR located close to the crest of the equatorial ionization anomaly (EIA) only experienced a faint positive storm-time effect around noon (12:00-14:00) UT hrs. It is important to note that despite the main phase spanned from daytime to night-time associated with a southward Bz and northward enhancement of IEFy, there is no significant differences in the TEC enhancement between the storm-time and mean quiet-time around (12:00-14:00) UT hrs at MAL2 and MBAR except a faint and short positive storm-time TEC around 13:00 UT. This seems to indicates that there could be some mechanisms inhibiting the uplift of ionospheric plasma transport to a height where production to loss ratio is high during the storm-time relative to the mean quiet-time, hence resulting to insignificant difference between the storm-time and mean quiet-time TEC. Dugassa et al. 2020a studied the ionospheric response of TEC over America, Africa and Asia using the 20 January 2016 geomagnetic storm. They found a positizve storm-time effect over Africa and American sector during the main phase which they associated to the southward turning of the Bz. The observation from the present study confirms the occurrence of positive storm-time effect during the main phase of the magnetic storm 17 March 2013 which we attributed to the resultant effect of prompt penetration electric field (PPEFs) that enhances the fountain effect during storm-time relative to the mean quiet-time.

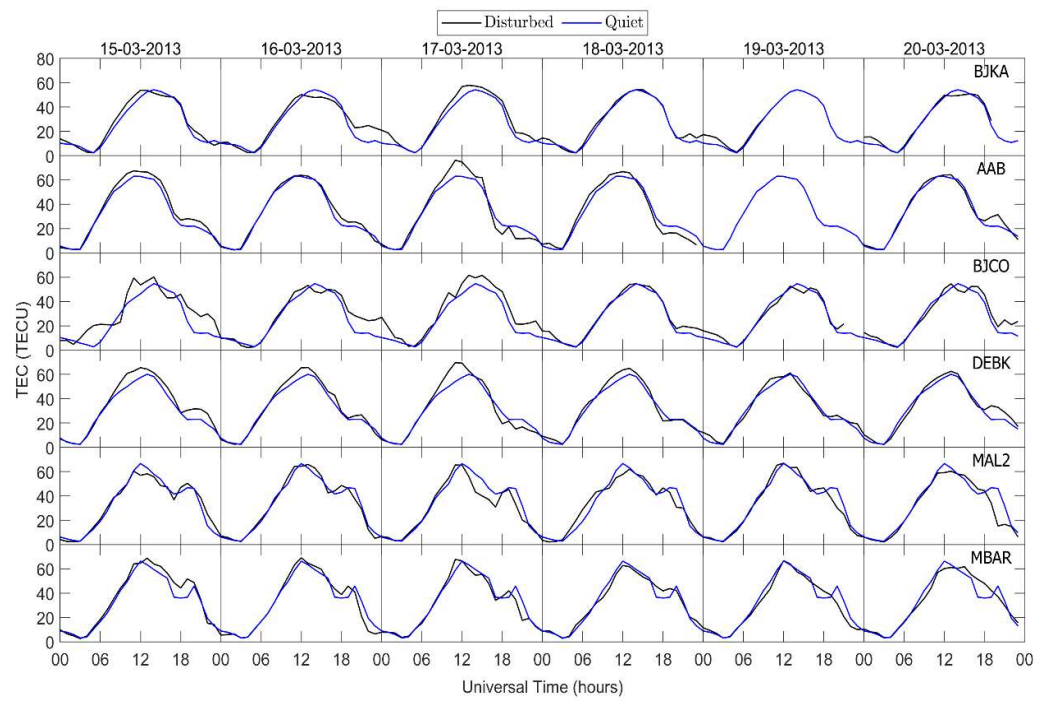


Figure 3 Diurnal variation of TEC during the 15-20 March, 2013 magnetic storms

During the recovery phase, faint positive storm-time effects are observed at BJKA, DEBK and MAL2 around (06:00-11:00) UT hrs on 18 March 2013. These positive storm-time effects were observed to slightly change to negative storm-time seen at BJCO and MBAR on 19-20 March 2013. Equal magnitude of storm-time and mean quiet time TEC are observed at AAB around (06:00-11:00) UT hrs during the recovery days. These findings are



consistent with earlier observation by Habyarimana et al., 2023.

The reason for the equal magnitude between the storm-time and mean quiet-time TEC around (06:00-11:00) UT hrs at some latitudes during the main and recovery phases may likely arise from the fact that the ionospheric transport mechanism could not influence significant deviation in the plasma distribution along the magnetic field lines. Despite significant energy deposition during the main and recovery phases, the equal magnitude of storm-time and mean quiet-time reflect insignificant deviation between the daytime DDEF and PPEF effect mostly during the recovery phase.

Also during the recovery phase, a faint positive storm-time effect is seen at AAB and DEBK latitudes seen around (12:00-14:00) UT hrs and changed to negative storm-time effect at MAL2 and MBAR throughout the recovery days. We assert that these variations demonstrate the effective distribution of ionization and the fountain effect during the recovery phase. The negative storm-time effect during the recovery phase is a strong evidence of predominance of ionospheric disturbance dynamo electric field (DDEF) suppressing the fountain effect during these particular periods. Hence, the magnetic storm-time effect observed around (06:00-11:00) UT hrs may be associated with the decrease in eastward electric field caused by overwhelming effect of the DDEF. The westward electric fields from the DDEF cause downward plasma motion that transport plasma to lower altitudes where fast molecular recombination lead to decrease in TEC Wang et al., 2013, Abdu, 1997, Sreeja et al., 2009. Habyarimana et al. 2023, Ren et al. 2020 observed similar daytime negative storm-time effect at MBAR and attributed it to ionospheric disturbance dynamo which exceeded the DP-2 current during this time.

## 3.2 The 1 June 2013 Geomagnetic storm event

Figure 4 shows the variations of interplanetary and geomagnetic field parameters from 28 May to 5 June 2013 in the following order from top to bottom: Bz, V, PSW, IEFy, Dst index and Ap and AE indices respectively. During these intervals of days, a moderate magnetic storm occurred on 1st June 2013 and this caused significant perturbations in the interplanetary and geomagnetic parameters across the globe. The storm was triggered by a combine effect of coronal mass ejections (CMEs) and high speed solar wind streams (HSSWS). The initial phase of the storm is marked by a sharp northward turning of Bz that reached ~ 9 nT around 24:00 UT as indicated in Figure 4 (panel a) signaling the compression of the outer magnetosphere as demonstrated by the sharp positive enhancement of dynamic pressure (see Figure 4 panel c). The northward turning of Bz is associated with southward turning of the IEFy with peak amplitude ~-4 mV/m as shown in Figure 4 (panel d). Other parameters also respond to the compressed state of the outer magnetosphere in various ways. The initial phase of the storm lasted for about 9 hrs spanning between 16:04 UT on 31 May 2012 and 01:15 UT on 01 June, 2013.

The main phase of the storm is characterized by a southward turning of Bz. The Bz remained strongly southward lasting for several hours as shown in Figure 4 (panel a). During the main phase, the Bz reached its minimum value -19 nT (see Figure 4 panel a) accompanied by a northward orientation of the IEFy which reached about 9.5 mV/m as shown in Figure 4 (panel d) on 1 June 2013. The southward orientation of Bz is associated with the prompt penetration electric field (under-shielding) which is eastward (westward) in the daytime (night-time) hours. The main phase demonstrates the effect of prompt penetration electric field (PPEFs) and magnetospheric currents known to dominate the main phase of a magnetic storm. Moreover, during the main phase, the V increased from ~400 km/s to about 680 km/s as shown in Figure 4 (panel b). The IEFy (panel d) and AE (panel g) and Ap index (panel f) shows significant perturbations suggesting possible higher energy deposition during the main phase.



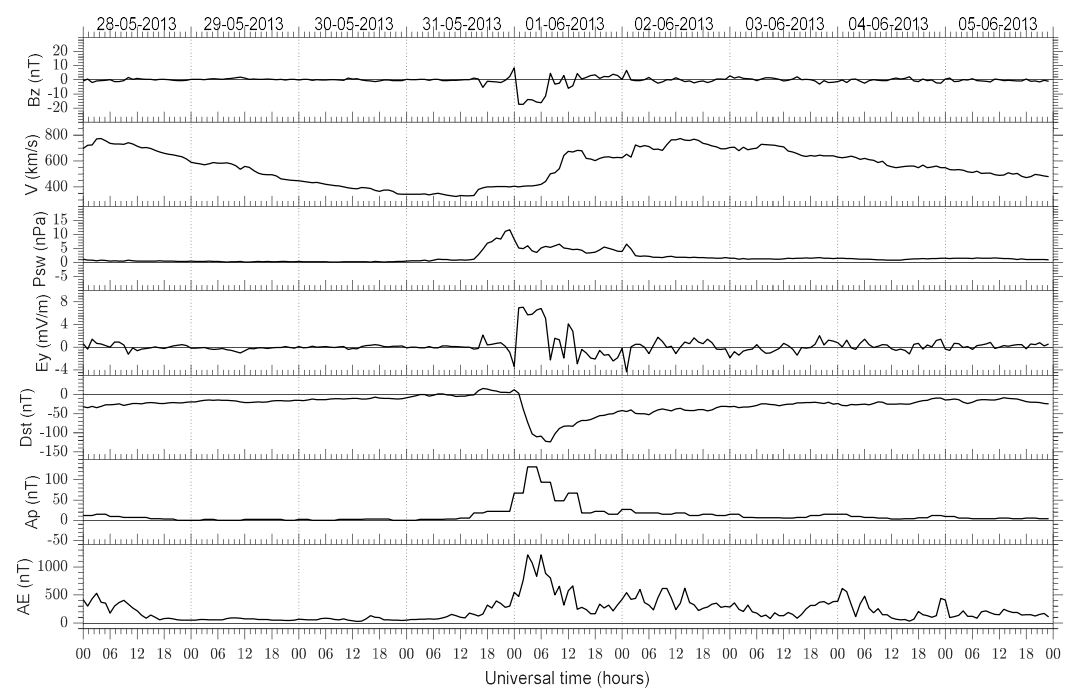


Figure 4 Interplanetary magnetic field, and and geomagnetic activity indices during the May 28 2013 to 5 June 2013 geomagnetic storm. From top to bottom are the interplanetary magnetic field (IMF) Bz, solar wind speed (V) dynamic pressure (PSW), Interplanetary electric field (IEFy), disturbance storm time (Dst), Ap index, and auroral electrojet (AE).

Following the main phase, the recovery phase of the storm is marked by the northward turning of Bz seen on 1 June 2013 and lasted for about 5 days. It started around 07:49 UT on 1 June 2013 to 15:50 UT on 5 June 2013. During the recovery phase, strong perturbations on the AE index seen in Figure 4 (panel g) and on the IEFy (panel d) indicates prompt penetration electric field (PPEFs) and other magnetospheric processes into the thermosphere-ionosphere even during the recovery phase of the storm of 1 June 2013. The recovery phase is associated with a prolong enhancement of V up to 775 km/s as illustrated in Figure 4 (panel b). Other parameters such as the dynamic pressure, (PSW), Dst index and Bz comes to their normal levels during the recovery phase of the storm but the V appeared higher than what was observed during the main phase (see Figure 4 panel b). The effect of the prolong higher V during the recovery phase will be discussed in subsequent sections.

## 3.4 Ionospheric Response to the 1 June 2013 Geomagnetic storm event

The storm-time diurnal TEC variations that occurred on 1 June 2013 and their comparison with mean quiet-time TEC obtained from the average of 3 quietest days are presented in Figure 5. For this magnetic storm, only days with  $Kp \le 4$  after the occurrence of the storm are used in the study. The storm-time TEC variations for AAB for the days 28-30 May 2013 are not available. On the day of the storm, (1 June 2013) AAB experienced a data gap possibly due to technical glitches. Prior to the occurrence of 1 June 2013 magnetic storm, the storm-time TEC do not show any significant deviations from the mean quiet-time TEC behavior noticeable between 06:00 and 11:00 UT hrs across all the latitudes.

Before the occurrence of the storm (28-30 May, 2013) around noon-dusk sector (12:00-17:00) UT hrs, a significant deviations are observed between storm-time and the mean quiet-time TEC variations that are prominent at BJKA latitude and appeared mild at BJCO latitudes only to appear stronger at MAL2 and MBAR as illustrated in Figure 5. During these periods (12:00-17:00) UT hrs, prominent positive storm-time effects are generated at BJK, DEBK, MAL2 and MBAR. These positive istorm-time effects are consequences of stronger fountain effect caused by intensed EXB plasma drift Fagundes et al., 2016; Blagoveshchensky et al., 2019. Similar effects are observed around (06:00-11:00) UT hrs across all the latitudes on the day of the SSC (31st May 2013). Exception to this is BJCO and AAB with negative and faint positive storm-time effect around (06:00-11:00) UT hrs. The main phase negative storm-time are consequences of weaker PPEF, hence ionospheric plasma drift could not be transported to a height with minimal loss rate. Also, on the day of the SSC (31st May 2013), a faint positive storm-time effect is seen around (12:00-17:00) UT hrs across all the latitudes exception of BJCO with a faint negative storm-time



effect. This indicates that for this magnetic storm, SSC that occurred around 16:00 UT on the 31<sup>st</sup> May 2013 seems to have only a mild effect on the TEC variations. This could possibly arise from the fact that at the time of the SSC, most of the stations are in their local night-time periods with electric field opposite to the zonal electric field (westward for night-time) and hence could not enhance the upward EXB plasma drift during the SSC. On the day of the SSC, a unique phase variations are observed between the storm-time TEC and mean quiet-time around (10:00-14:00) UT hrs at MAL2 and MBAR which is believed to arise from significant deviations in the electrodynamic processes between the storm-time and mean quiet-time TEC.

During the main phase, the storm-time TEC exhibit similar variation with almost equal magnitude around (06:00-11:00) UT hrs observed only at BJKA latitude. Other latitudes exhibit faint negative storm-time effect conspicuously seen at AAB, DEBK and MAL2 around (06:00-11:00) UT hrs on 1st June 2013. Although, the main phase of the magnetic storm occur during the time most of the stations are in their post-midnight to dawn sector characterized by night-time westward (eastward) PPEFs (DDEFs) and a daytime eatward (westward) PPEFs (DDEFs) which modifies the structure of TEC. This could possibly be the reason for the faint negative storm-time effect across most of the latitudes with no appreciable difference between the storm-time and mean quiet-time TEC at BJKA around (06:00-11:00) UT hrs on 1 June 2013. Summarily, these negative storm-time effects are consequences of weaker fountain effect caused by westward electric field. During the noon-dusk sector (12:00-17:00) UT hrs, the storm-time TEC magnitude appeared greater than the mean quiet-time which is more prominent at BJKA and DEBK and this generates positive storm-time effect at these latitudes.

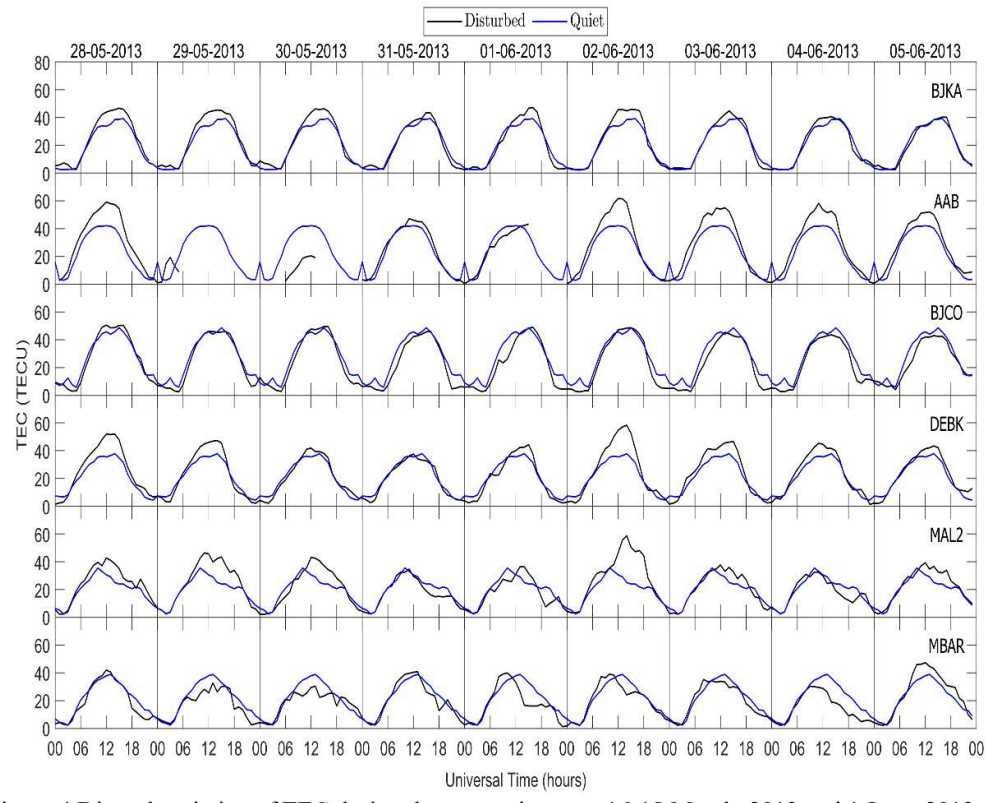


Figure 4 Diurnal variation of TEC during the magnetic storm 16-18 March, 2013 and 1 June, 2013

The consistent positive storm-time TEC variations during the main phase around (12:00-17:00) UT hrs is consistent with the higher energy deposition at high latitudes that cause prompt penetration electric field which then intensifies the zonal electric field- a process that uplift the low latitude plasma to higher altitudes where production to loss ratio is high Rishbeth, 1998. We suspect that the faint positive storm-time effect observed around noon-dusk sector (12:00-17:00) UT hrs of the present study could be due to weakening effect of PPEFs during the dawn sector.

The prevailing positive storm-time effect observed during the main phase of the storm could be attributed to the stronger presence of PPEF that enhances the upward EXB plasma drift as previously observed by research workers



e.g., Balan et al., 2010. Other mechanisms have been pointed as the cause of positive ionospheric storm. For instance, earlier effort by research workers have suggested that the occurrence of positive storm-time effect results from the enhancement in the equator-ward neutral winds arising from the high latitude energy deposition Prolss, 1995. During geomagnetic storm, the presence of enhanced energy deposition at higher latitudes penetrates to the low latitude resulting in the vertical redistribution of plasma Schunk and Nagy, 2000 which lead to a decrease in the loss rate of electrons and thus cause a relative increase in storm-time TEC relative to the mean quiet-time. During the recovery phase marked by the southward reduction in Bz and Dst index as shown in Figure 4 (panels a and c) from 2 to 5 June, 2013, the storm-time TEC amplitude appeared slightly higher than the mean quiet-time TEC magnitude around (06:00-11:00) UT hrs observed at AAB, DEBK and MBAR while reverse is the case at BJCO latitude. On the other hand, BJKA exhibit almost equal magnitude around (06:00-11:00) UT hrs during the recovery phase.

During the recovery phase when the ionospheric disturbance dynamo mechanism is very active generating daytime westward electric field that causes downward plasma motion to low altitudes where molecular recombination decreases plasma densities and this lead to decrease in TEC, however, a positive storm-time effect is observed at BJKA, BJCO and AAB latitude. As illustrated by the magnetic and interplanetary parameters, the positive storm-time effect observed at some latitudes of this present study during the recovery days is associated to an intense energy deposition into the auroral region which actively penetrates to the equatorial-low latitudes strengthening the upward transport of EXB plasma drift where molecular recombination is low and thus generate enhance TEC as obvious at AAB latitude of this study.

#### 4. Conclusion

- 1. During the SSC, The storm-time TEC does not show any significant deviation from the quiet-time TEC indication of possible mechanism inhibiting the uplift of plasma transport to a height where production to loss ratio is high.
- 2. The negative storm-time effect during the recovery phase is a strong evidence of predominance of ionospheric disturbance dynamo electric field (DDEF) suppressing the fountain effect during these particular periods.
- 3. The main phase negative storm-time are consequences of weaker PPEF, hence ionospheric plasma drift could not be transported to a height with minimal loss rate.
- 4. The prevailing positive storm-time effect observed during the main phase of the storm could be attributed to the stronger presence of PPEF that enhances the upward EXB plasma drift
- 5. The two moderate magnetic storm events considered in this study reveal that the positive storm-time effect during the main and recovery phase is mainly associated with the induced electric field disturbances.
- 6. For the magnetic storm event (1st June 2013), during the recovery phase, significant day-time positive storm-time effect were observed across some latitudes that are larger than the main phase of the storm.

## References

- Abdu, M. A.; Sobral, J. H. A., De Paula, E. R., and Batista, I. S. Magnetospheric disturbance effects on the equatorial ionization anomaly (EIA): An overview. J. Atmos. Sol. Terr. Phys. 1991, 53, 757–771.
- Abdu, M.A., Major phenomena of the equatorial ionospherethermosphere system under disturbed conditions. J. Atmos. Sol. Terr. Phys. 59, 1505–1519, 1997 https://doi.org/10.1016/S1364-6826(96)00152-6.
- Akala, A. O., Oyeyemi, E. O., Amaechi, P. O., Radicella, S. M., Nava, B., and Amory-Mazaudier, C. Longitudinal responses of the equatorial/low-latitude ionosphere over the oceanic regions to geomagnetic storms of May and September 2017. *Journal of Geophysical Research: Space Physics, 125*, e2020JA0279 63, 2020.
- Balan, N., Alleyne, H., Otsuka, Y., Vijaya, L. D., Fejer, B. G., and McCrea, I., Relative effects of electric field and neutral wind on positive ionospheric storms. *Earth Planet Space*, 61(4), 439-445, 2009. <a href="https://doi.org/10.1186/BF03353160">https://doi.org/10.1186/BF03353160</a>
- Blagoveshchensky, D. V., Sergeeva, Maria A., and Shmelev, Y. A. TEC dynamics during the intense magnetic storm, 2019.
- Blanc, M., and Richmond, A. D., The ionospheric disturbance dynamo. J. Geophys. Res.,1669–1686, 1980. doi:10.1029/JA085iA04p01669
- Dugassa, T., Habarulema, J. B., Nigussie, M. Equatorial and lowlatitude ionospheric TEC response to CIR-driven geomagnetic storms at different longitude sectors. Adv. Space Res. 66 (8), 1947–1966, 2020a
- Fagundes, P. R., Cardoso, F. A., Fejer, B. G., Venkatesh, K., Ribeiro, B. G., and Pillat, V. G. Positive and negative GPS-TEC ionospheric storm effects during the extreme space weather event of March 2015 over the Brazilian sector, J. Geophys. Res. Space Physics, 121, 5613–5625, 2016. doi:10.1002/2015JA022214.



- Fejer, B. G., Kelley, M. C., Senior, C., de la Beaujardiere, O., Holt, J. A., Tepley, C. A., Burnside, R., Abdu, M. A., Sobral, J. H. A., Woodman, R. F., Kamide, Y., Lepping, R. Low- and mid-latitude ionospheric electric fields during the January 1984 GISMOS Campaign. 1990. https://doi.org/10.1029/JA 095iA03p02367
- Gopi Krishna Seemala. Estimation of ionospheric total electron content (tec) from gnss observations, in: Atmospheric Remote Sensing, Elsevier, pp. 63–84, 2023
- Gonzalez, W. D., Joselyn, J. A., Kamide, Y., Kroehl, H. W., Rostoker, G., Tsurutani, B. T., & Vasyliunas, V. M. What is a geomagnetic storm? *Journal of Geophysical Research*, 99, 5771–5792, 1994, https://doi.org/10.1029/93JA02867
- Huang, C. S., J. C. Foster, J. C Goncharenko, L. P., Erickson, P. J., Rideout, W and Coster, A, J. A strong positive phase of ionospheric storms observed by the Millstone Hill incoherent scatter radar and global GPS network, J. Geophys. Res., 110, A06303, 2005, doi:10.1029/2004JA010865
- Kikuchi, T., Hashimoto, K. K., and Nozaki, K., 2008. Penetration of magnetospheric electric fields to the equator during a geomagnetic storm. J. Geophys. Res., 113, A06214, 605m 2008, doi:10.1029/2007JA012628.
- Kamide, Y., Yokoyama, N., Gonzalez, W., Tsurutani, B. T., Daglis, I. A., Brekke, A., Masuda, S. Two-step development of geomagnetic storms. *J. Geophys. Res.* 103 (A4), 6917–69211,1998.
- Laura A. Hayes, Peter T. Gallagher, Joseph McCauley, Brian R. Dennis, Jack Ireland, Andrew Inglis, Pulsations in the Earth's lower ionosphere synchronized with solar flare emission, *J. Geophys. Res. Space Phys.* 122 (10) (2017) 9841–9847.
- Liu J, Zhao B and Liu, L 2010 Time delay and duration of ionospheric total electron content responses to geomagnetic disturbances; *Ann. Geophys.* 28 795–805, doi: 10.5194/angeo-28-795-2010, 2010
- Lin, C. H, Richmond, A. D. Heelis, R. A. Bailey, G. J. Lu, G. Liu, J. Y. Yeh, H. C. Su, S. Y. Theoretical study of the low-and midlatitude ionospheric electron density enhancement during the October 2003 superstorm: Relative importance of the neutral wind and the electric field. *J. Geophys. Res. Space Phys.* 2005, 110, 1– 14.
- Moore, T, E, Peterson, W, K., Russell, C, T., Chandler, M, O, Collier, M, R., Collin, H, L., Craven, P, Fitzenreiter, D, R., Giles, B, L., Pollock, C, J. Ionospheric mass ejection in response to a cme, *Geophys. Res. Lett.* 26 (15) (1999) 2339–2342.
- Mustapha, A., Furfuri, M. I., Kaoje, M. B., & Mohammed, M. Characterization of Equatorial Ionization Anomaly at the African Southern Hemisphere During a High Solar Activity Period. *International Astronomy and Astrophysics Research Journal*, 6(1), 102-114, 2024
- Imtiaz, N Waqar, Y, and Majid, K. Response of the low-to mid-latitude ionosphere to the geomagnetic storm of September 2017, in Annales Geophysicae, vol. 38, Copernicus GmbH, 2020, pp. 359–372, 2017
- Nishida, A. Geomagnetic DP2 fluctuations and associated magnetosphericphenomena. J. Geophys. Res. 73 (5), 1795–1803, 1968
- Prolss, G. W. (1995). Ionospheric f-region storms. In H. Volland (Ed.), *Handbook of atmospheric electrodynamics* (pp. 195–248). Boca Raton, Fla.: .CRC Press.
- Schunk, R. W., and A. F. Nagy (2000), Ionospheres: Physics, Plasma Physics, and Chemistry, Cambridge Univ. Press, New York.
- Sreeja, V., S. Ravindran, T. K. Pant, C. V. Devasia, and L. J. Paxton (2009), Equatorial and low latitude ionosphere thermosphere system response to the space weather event of August 2005, J. Geophys. Res., 114, A12307, doi:10.1029/2009JA014491.
- Rastogi, R. G., & Klobuchar, J. A. (1990). Ionospheric electron content within the equatorial F2 layer anomaly belt. *Journal of Geophysical Research*, 95, 19,045–19,052. doi:10.1029/ JA095iA11p19045
- Richmond A. D, G. Lu, G (2000). Upper-atmospheric effects of magnetic storms: a brief tutorial, J. Atmos. Sol.-Terr. Phys. 62 (12), 1115–1127.
- Rishbeth, H. (1998). How the thermospheric circulation affects the ionospheric F2-layer. *Journal of Atmospheric and Solar- Terrestrial Physics*, 60, 1385–1402.
- Ren D, Lei J, Zhou S, Li W, Huang F, Luan X, Dang T, Liu Y (2020) Highspeed solar wind imprints on the ionosphere during the recovery phase of the August 2018 geomagnetic storm. Space Weather 18(7):e2020SW002480
- Sastri, J. H., Ramesh, K. B., and Rao, H. N. R., 1992. Transient composite electric field disturbances near the dip equator associated with auroral sub-storms. *Geophys. Res. Lett.*, 19, 1451–1454, doi:10.1029/92GL01447
- Seemala, G. K., Valladares, C. E., 2011. Statistics of total electron content depletions observed over the South American continent for the year 2008. Radio Sci. 46, RS5019,doi:10.1029/2011RS004722
- Spiro, R.W., R.A. Wolf, and B.G. Fejer (1988), Penetration of high-latitude-electric field effects to low latitudes during SUNDIAL 1984, *Ann. Geophys.* **6**, 39-49
- Wang, W., Lei, J. Burns, A, G, Solomon, S, C, Wiltberger, M, Xu, J, Zhang, Y, Paxton, Lm and Coster, A. Ionospheric response to the initial phase of geomagnetic storms: Common features, J. Geophys. Res., 115, A07321, 2010, doi:10.1029/2009JA014461.